

Theoretical investigation of the conformation and hydrogen bonding ability of 5-arylazosalicylaldoximes

A. Manimekalai*, R. Balachander

Department of Chemistry, Annamalai University, Annamalainagar, Chidambaram 608 002, Tamilnadu, India

HIGHLIGHTS

- ▶ Conformations of oximes have been predicted from spectral and theoretical studies.
- ▶ Intramolecular hydrogen bonding in oximes and aldehydes.
- ▶ Molecular properties for oximes and aldehydes were determined from computational studies.

ARTICLE INFO

Article history:

Received 24 November 2011
 Received in revised form 1 April 2012
 Accepted 1 June 2012
 Available online 12 June 2012

Keywords:

5-Arylazosalicylaldoximes
 Hydrogen bonding
 Computational studies

ABSTRACT

Conformations of 5-arylazosalicylaldoximes **6–10** have been predicted from spectral and theoretical studies. The orientation of OH bond is predicted to be *anti* to C=N bond from the PES analysis. The presence of intramolecular hydrogen bonding in oximes **6–10** and their parent aldehydes **1–5** is supported by the additional bond and ring critical points from AIM analysis, hyperconjugative interaction energies determined from NBO analysis and selected geometrical parameters derived from optimized structures. Molecular properties such as dipole moment, polarizability and hyperpolarizabilities for oximes **6–10** and their parent aldehydes **1–5** were also determined by computational studies.

Crown Copyright © 2012 Published by Elsevier B.V. All rights reserved.

1. Introduction

The azobenzene chromophore has elicited considerable interest because of its novel photoisomerization and photocyclization reactions [1] as well as its technological applications in the dye and pigment industry [2]. Their oxidation–reduction behavior play important role in biological activity [3,4]. Some of the photoreponsive azobenzene derivatives show enhanced transport of metal ions across a liquid membrane on irradiation [5,6]. Derivatives of azobenzene can be used as intermediates as well as ligands to synthesize several organic compounds and coordination complexes [7–10]. Generally organic chromophores and polymers are strongly fluorescent in dilute solution and aggregate formation leads to reduction in fluorescent efficiency in the solid state. However an asymmetric disulfide compound consisting of a photoisomerizable azobenzene unit coupled to a biphenyl fluorophore [11] whose isolated species is weakly fluorescent in initial solution, spontaneously self-assembles into strongly fluorescent aggregates under UV light irradiation. Several reports in literature reveal enhancement of fluorescence [12,13] and photoreactivity [14,15]

from self-assembled aggregates of azo benzene units. Incorporation of azobenzene in bilayer assemblies exhibit novel photochemical reactivity and energy transfer on excitation [16]. The photochemical behavior and energy transfer of azobenzene derivatives in microphorous crystals have also been reported in literature [17–21].

Second-order non-linear optical materials consisting of azo dyes poled in polymer matrices have been synthesized and their NLO behavior was studied in detail [22,23]. Azobenzene dendrimers with a branch point at each of the donor–acceptor functionalized azobenzene monomeric units, have large first hyperpolarizabilities [24–26] and quantum chemical calculations have also been made to predict interaction in various conformations between monomeric unit of donor–acceptor functionalized azobenzene dendrimers [27]. Because of the wide applicability of azobenzene derivatives we thought that synthesis and characterization of some simple azo derivatives is of considerable importance and hence the study has been carried out. In the present study five 5-arylazosalicylaldoximes **6–10** were synthesized and their conformations have been predicted from spectral and theoretical studies. Single crystal measurements made for 5-*p*-tolylazosalicylaldoxime **7** also predict the same conformation derived from computational studies. The presence of intramolecular

* Corresponding author. Tel.: +91 9486283468.

E-mail address: profmekal1@gmail.com (A. Manimekalai).

hydrogen bonding in oximes **6–10** and their parent aldehydes **1–5** is evidenced from AIM, NBO and selected geometrical properties.

2. Experimental

2.1. Synthesis of 5-arylazosalicylaldoximes **6–10**

5-Arylazosalicylaldehydes **1–5** were prepared according to the procedure reported by Odabasoglu et al. [28]. A mixture of 5-arylazosalicylaldehyde (1 mmol) and sodium acetate (0.5 g) was dissolved in boiling ethanol and hydroxylamine hydrochloride (0.13 g; 2 mmol) was added. The mixture was refluxed for 3 h. The reaction mixture was poured into water. The 5-arylazosalicylaldoxime separated out was filtered and recrystallized from ethanol. (**6**) aryl = phenyl, m.p. 153 °C, yield 70%; (**7**) aryl = *p*-tolyl, m.p. 155 °C, yield 70%; (**8**) aryl = *p*-methoxyphenyl, m.p. 160 °C, yield 75%; (**9**) aryl = *p*-fluorophenyl, m.p. 175 °C, yield 75% and (**10**) aryl = *p*-nitrophenyl, m.p. 180 °C, yield 70%.

2.2. Spectral measurements

The proton spectra at 500 MHz and proton decoupled ^{13}C NMR spectra at 125 MHz were recorded at room temperature on DRX 500 NMR spectrometer using 10 mm sample tube. Samples were prepared by dissolving about 10 mg of the sample in 0.5 mL of DMSO- d_6 containing 1% TMS for ^1H and 0.5 g of the sample in 2.5 mL of DMSO- d_6 containing a few drops of TMS for ^{13}C . The solvent chloroform- d also provided the internal field frequency lock signal. The ^1H – ^1H and ^1H – ^{13}C COSY spectra were performed on a DRX-500 NMR spectrometer. Avatar-330 FT-IR spectrophotometer was used for recording IR spectra (KBr pellet). For the parent aldehydes NMR spectra were recorded in chloroform- d .

2.3. Computational study

Geometry optimizations were carried out according to density functional theory available in Gaussian-03 package using B3LYP/6-31G(d,p) basis set [29] for the structures of oximes and their parent aldehydes. The polarizabilities and hyperpolarizabilities were determined from the DFT optimized structures by finite field approach using B3LYP/6-31G* basis set available in Gaussian-03 package and NBO calculations using the basis set B3LYP/6-31G(d,p) and B3LYP/6-311+G(d,p). AIM parameters were determined using AIM-All package [30] from B3LYP/6-31G(d,p) optimized structures.

2.4. X-ray analysis

Single crystal measurements of oxime **7** with the dimensions $0.30 \times 0.20 \times 0.15$ mm was chosen for X-ray diffraction study. Crystallographic measurements were done at 293(2) K with Bruker axis Kappa CCD diffractometer using graphite monochromated Mo K α radiation ($\lambda = 0.71073$ Å). The crystal structure was solved by direct method and refined by full-matrix least square technique on F^2 using the SHELX-97 set of program [31]. The parameters in the CIF form are available as [Electronic Supplementary Information](#) from the Cambridge Crystallographic Database Centre (CCDC 853941).

3. Results and discussion

5-Phenylazosalicylaldoxime (**6**), 5-*p*-tolylazosalicylaldoxime (**7**), 5-*p*-methoxyphenylazosalicylaldoxime (**8**), 5-*p*-fluorophenylazosalicylaldoxime (**9**) and 5-*p*-nitrophenylazosalicylaldoxime (**10**) were synthesized according to the [Scheme 1](#) and characterized by IR, ^1H and

^{13}C NMR spectroscopy. ^1H – ^1H , ^1H – ^{13}C COSY spectra and one-dimensional NMR spectra were recorded in DMSO- d_6 due to poor solubility of the compounds in CDCl_3 and analyzed. Odabasoglu et al. [28] have recorded ^1H and ^{13}C NMR spectra for the parent aldehydes **1, 2, 4** and **5** at 200 MHz in CDCl_3 . In the present study spectra were also recorded for the parent aldehydes **1–5** in CDCl_3 at 500 MHz.

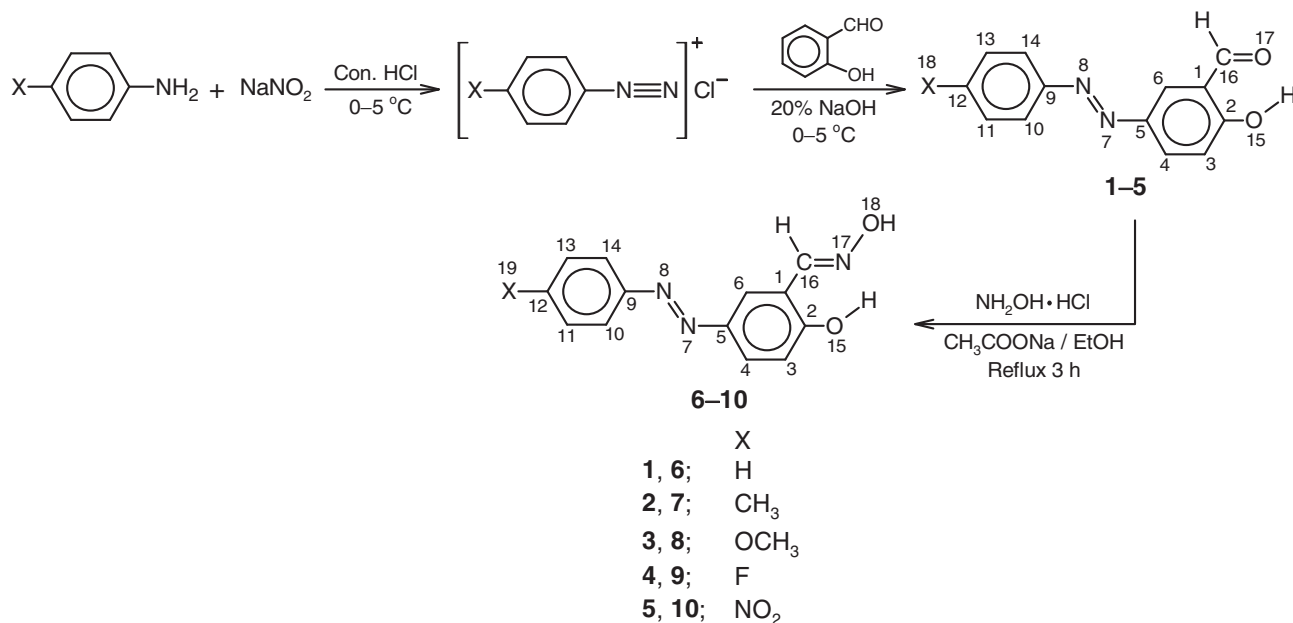
3.1. IR spectral analysis

The sharp peaks around 1610 cm^{-1} in the IR spectra of **6–10** are due to $\nu_{\text{C}=\text{N}}$ group. The stretching vibration of the OH (ν_{OH}) group was observed in the region 3410 cm^{-1} . Aromatic C=C stretching vibrations are seen around 1580 and 1500 cm^{-1} . The out of plane bending vibration of OH group appeared around 1390 cm^{-1} . The peaks around 1200 cm^{-1} are due to $\nu_{\text{C}-\text{O}}$ mode. Aromatic C–H out of plane bending vibrations appeared around 800 and 750 cm^{-1} . Strong peaks for N=N group were observed around 1260 cm^{-1} . Aromatic C–H stretching vibration was appeared around 3060 cm^{-1} . The sharp peaks around 1010 cm^{-1} are due to $\nu_{\text{N}-\text{O}}$ mode. In oxime **10** peaks for ν_{NO_2} appeared at 1520 and 1338 cm^{-1} . The IR data of **6–10** are listed in [Table 1](#).

3.2. NMR spectral analysis

The signals in the ^1H NMR spectra were assigned based on their positions, integrals and multiplicities and confirmed by the correlations observed in the COSY spectra. The two high frequency singlets observed at 11.51 and 10.89 ppm in **6** are assigned to phenolic proton H(15) and oxime OH proton H(18) respectively. The signal at 8.43 ppm is assigned to H(16) proton. The low frequency doublet observed at 7.10 ppm ($J = 8.5$ Hz) is assigned to the *ortho* proton with respect to OH group i.e., H(3). For H(6), a doublet (*meta* coupling of $J = 2.5$ Hz) at 8.14 ppm was observed. The ^1H NMR spectrum further reveals two triplets at 7.58 and 7.53 ppm (integral corresponds to three protons) and a doublet at 7.86 ppm with spacing 8.00 Hz (integral corresponds to three protons) for the aromatic protons of phenyl ring and for the proton H(4). The high intense triplet at 7.58 ppm is obviously due to the *meta* protons of the phenyl ring i.e., H(11) and H(13). The remaining triplet at 7.53 ppm is due to *para* proton of the phenyl ring i.e., H(12). The doublet at 7.86 ppm is therefore assigned to H(4) proton and *ortho* protons of the phenyl ring [H(10) and H(14)]. This assignment is further confirmed by the correlations observed in the ^1H – ^1H COSY spectrum. In a similar manner assignments were done for other oximes and their parent aldehydes.

In ^{13}C NMR spectra quaternary carbons can be easily distinguished from other carbons based on small intensities. Assignments of the aromatic ring carbons were made on the basis of cross peaks observed in ^1H – ^{13}C COSY spectra. The downfield signal at 146.51 ppm in the oxime **6** is assigned to $-\text{C}=\text{N}$ carbon. The hydroxy bearing carbon [C(2)] resonates at 159.34 ppm. For the *ipso* carbons C(1), C(5) and C(9) signals were observed at 119.73, 145.60 and 152.45 ppm. Among these signals the low frequency signal at 119.73 ppm is assigned to the quaternary carbon C(1) since it is *ortho* with respect to electron releasing OH group. Among the remaining signals at 145.60 and 152.45 ppm, the signal at 152.45 ppm is assigned to the *ipso* carbon C(9) which is attached to the nitrogen atom N(8). Obviously, the signal at 145.60 ppm is due to C(5) which is *para* with respect to OH group. The low frequency signal at 117.31 ppm is assigned to C(3) carbon and this assignment is based on the known shielding magnitude of OH group. The C(4) and C(6) carbons resonate at 125.84 and 122.34 ppm respectively. From the intensities, the signals at 122.70 and 129.85 ppm are assigned to *ortho* [C(10) and C(14)] and *meta* [C(11) and C(13)] carbons and the signal at 131.30 ppm is assigned to *para* carbon [C(12)]. In a similar manner assignments



Scheme 1. Structures of synthesized compounds and synthetic steps adopted.

Table 1
IR spectral data (cm⁻¹) of **6–10**.

Assignments	6	7	8	9	10
O–H	3414	3189	3415	3429	3370
C–H (aromatic)	3060	3095	3107	2923	3103
C=N	1622	1601	1625	1619	1615
C=C	1574	1577	1589	1574	1579
	1485	1497	1493	1487	1487
OH	1392	1386	1393	1391	1387
N=N	1265	1256	1228	1262	1271
C–O	1195	1154	1269	1158	1103
N–O	1013	1021	1015	1004	1011
Aromatic CH out of plane bending vibration	785	834	842	824	859
	761	769	779	682	751
	685	–	–	–	–
NO ₂	–	–	–	–	1517
					1338

Table 2
¹H NMR chemical shifts (ppm) of oximes (DMSO-*d*₆) **6–10** and their parent aldehydes (CDCl₃) **1–5**.

Comps.	H-3	H-4	H-6	H-16	H-15	H-18	H-19	H-10 and H-14	H-11 and H-13	H-12
6	7.10 (d, 8.50 Hz)	7.86	8.14 (d, 2.50 Hz)	8.43	11.51	10.89	–	7.86	7.58 (d)	7.53 (t)
7	7.08 (d, 10.00 Hz)	7.81 (dd, 2.50, 8.50 Hz)	8.11 (s)	8.43	11.46	11.46	2.40	7.75	7.37	–
8	7.07 (d, 9.00 Hz)	7.80 (dd, 2.25, 8.75 Hz)	8.08 (d, 2.50 Hz)	8.43	11.49	10.78	3.86	7.85	7.11	–
9	7.09 (d, 9.00 Hz)	7.84 (dd, 2.50, 8.50 Hz)	8.13 (d, 2.50 Hz)	8.43	11.51	10.89	–	7.93–7.90	7.41	–
10	7.13 (d, 9.00 Hz)	7.93 (dd, 2.50, 8.75 Hz)	8.21 (d, 2.50 Hz)	8.42	11.55	11.15	–	8.04	8.41	–
1	7.16 (d, 8.50 Hz)	8.21 (dd, 2.50, 9.00 Hz)	8.24 (d, 2.50 Hz)	10.07	11.34	–	–	7.94–7.92	7.57–7.53	7.52–7.49
	(7.19)	(8.08)	(8.17)	(10.36)	(11.51)	–	–	(7.85)	(7.57)	(7.56)
2	7.15 (d, 8.50 Hz)	8.19 (dd, 2.50, 9.00 Hz)	8.21 (d, 2.00 Hz)	10.06	11.32	2.47	–	7.85–7.82	7.36–7.34	–
	(7.16)	(8.04)	(8.13)	(10.34)	(11.29)	(2.36)	–	(7.73)	(7.34)	–
3	7.13 (d, 9.00 Hz)	8.16 (dd, 2.00, 8.50 Hz)	8.17 (d, 2.00 Hz)	10.04	11.29	3.92	–	7.93–7.92	7.05–7.04	–
4	7.15(d, 9.00 Hz)	8.19 (dd, 2.25, 8.50 Hz)	8.22 (d, 2.50 Hz)	10.06	11.35	–	–	7.96–7.94	7.25–7.21	–
	(7.18)	(8.06)	(8.16)	(10.35)	(11.54)	–	–	(7.92)	(7.40)	–
5	7.19 (d, 8.50 Hz)	8.25 (dd, 2.25, 8.50 Hz)	8.31 (d, 2.00 Hz)	10.08	11.48	–	–	8.05	8.42	–
	(7.19)	(8.09)	(8.18)	(10.33)	(11.46)	–	–	(7.98)	(8.37)	–

Values within parentheses are taken from Ref. [28] for aldehydes **1, 2, 4** and **5**.

were made for other compounds **7–10** and their parent aldehydes. The ¹H and ¹³C chemical shifts obtained in this manner are listed in Tables 2 and 3 respectively.

3.3. Conformational analysis

There are four possible conformations for the oximes as shown in Fig. 1. In conformation **A** intramolecular hydrogen bonding ex-

Table 3
 ^{13}C NMR chemical shifts (ppm) of oximes (DMSO- d_6) **6–10** and their parent aldehydes (CDCl_3) **1–5**.

Compds.	C-3	C-4	C-6	C-16	C-19/ C-18	C-1	C-2	C-5	C-9	C-12	C-10 and C-14	C-11 and C-13
6	117.31	125.84	122.34	146.51	–	119.73	159.34	145.60	152.45	131.30	122.70	129.85
7	117.37	125.71	122.68	146.58	21.44	119.72	159.58	145.40	150.55	141.30	122.68	130.34
8	117.22	125.45	121.97	146.63	56.05	119.58	158.75	145.63	146.71	161.95	115.00	124.59
9	117.32	125.84	122.28	146.41	–	119.76	162.88	149.21	159.35	164.86	124.93	116.71
10	117.54	126.63	122.99	146.08	–	120.08	155.84	145.69	148.46	160.56	125.51	145.69
1	118.59 (118.26)	130.71 (123.86)	129.33 (129.47)	196.57 (187.36)	– (187.36)	120.32 (122.48)	167.77 (163.09)	145.94 (144.78)	152.38 (151.80)	131.07 (130.88)	123.61 (122.18)	129.17 (129.21)
2	118.52 (118.29)	122.59 (123.72)	129.04 (129.52)	196.59 (187.43)	21.51 (20.91)	121.06 (122.53)	163.54 (162.97)	146.01 (144.88)	150.49 (149.96)	141.69 (141.22)	122.77 (122.29)	129.75 (129.83)
3	118.46	128.71	124.66	196.61	55.61	120.33	162.13	146.05	146.73	163.25	114.31	130.60
4	116.23 (118.27)	124.73 (123.89)	129.32 (129.49)	196.51 (187.56)	–	120.31 (122.51)	163.79 (163.15)	145.76 (144.65)	148.91 (148.53)	165.39 (163.40)	124.80 (124.48)	118.63 (116.18)
5	118.99 (118.58)	130.65 (124.93)	130.68 (129.93)	196.37 (187.93)	–	120.37 (122.74)	155.52 (164.26)	145.77 (144.84)	148.72 (155.16)	164.87 (148.13)	123.36 (123.18)	124.81 (123.19)

Values within parentheses are taken from Ref. [28] for aldehydes **1**, **2**, **4** and **5**.

ists between hydroxyl proton and oxime nitrogen and hence it is stabilized over the other conformers in which there is no such hydrogen bonding. Further single crystal measurements were made for the oxime **7** and it also reveals the stable conformation as 'A' only. The ORTEP structure and close packed diagram for **7** are shown in Fig. 2.

Crystal data

$\text{C}_{14}\text{H}_{13}\text{N}_3\text{O}_2$

$M_r = 255.27$

Monoclinic, $P21/n$

$a = 13.7543(7) \text{ \AA}$

$b = 4.6276(2) \text{ \AA}$

$c = 19.0577(10) \text{ \AA}$

$\beta = 90.170(2)^\circ$

$V = 1213.01(10) \text{ \AA}^3$

$Z = 4$

Mo $K\alpha$ radiation

$\mu = 0.097 \text{ mm}^{-1}$

$T = 293(2) \text{ K}$

$0.30 \times 0.20 \times 0.15 \text{ mm}$

In order to confirm the favoured conformation computational calculations (geometry optimizations) were performed for the oxime **6** according to DFT method using B3LYP/6-31G(d,p) basis set available in Gaussian-03 package [29] for the four possible conformations and the relative energies determined are found to be 0.0 (A), 9.76 (B), 10.39 (C) and 7.98 (D) kcal mol $^{-1}$. Thus, the theoretical study predicts the favoured conformation as 'A' only. For other oximes also one can expect conformation 'A' as the favoured conformation.

For the oxime **8** in the favoured conformation 'A' there are two possible orientations of methoxy group as shown in Fig. 3. In conformation A, the methoxy methyl group is *anti* to N=N bond whereas in A' it is *syn*. Theoretical study [relative energies are 0.0 (A) and 0.22 (A') kcal mol $^{-1}$] predicts the favoured conformation as 'A' only for the oxime **8**. For the aldehydes **1–5** also there are four possible conformations as shown in Fig. 4. The relative energies determined by computational method for aldehyde **1** are found to be 0.0 (A), 13.74 (B), 12.17 (C) and 10.04 (D) kcal mol $^{-1}$. Thus, the theoretical study predicts the favoured conformation 'A' only for the aldehydes. To investigate the barrier for isomerisation process in the favoured conformation 'A' in aldehydes **1–5**, potential energy scan over C(1)–C(16) bond was carried out for a representative aldehyde **1**. The torsional angle C(6)–C(1)–C(16)–O(17) was varied in steps of 15° from 0° to 180° and the potential energy scan (PES) diagram is reproduced in Fig. 5. The barrier for the isomerisation process is predicted to be 22.38 kcal mol $^{-1}$.

Potential energy scan over N–O bond was also carried out to predict the orientation of OH group of oxime moiety in conformation A. The torsional angle C(16)–N(17)–O(18)–H(18) was varied in steps of 10° from 0° to 180° and PES diagram thus obtained is illustrated in Fig. 6. From the scan diagram, it is concluded that O–H bond is *anti* to C=N bond [C(16)–N(17)–O(18)–H(18) = 180°] and this arrangement is favoured over the *syn*

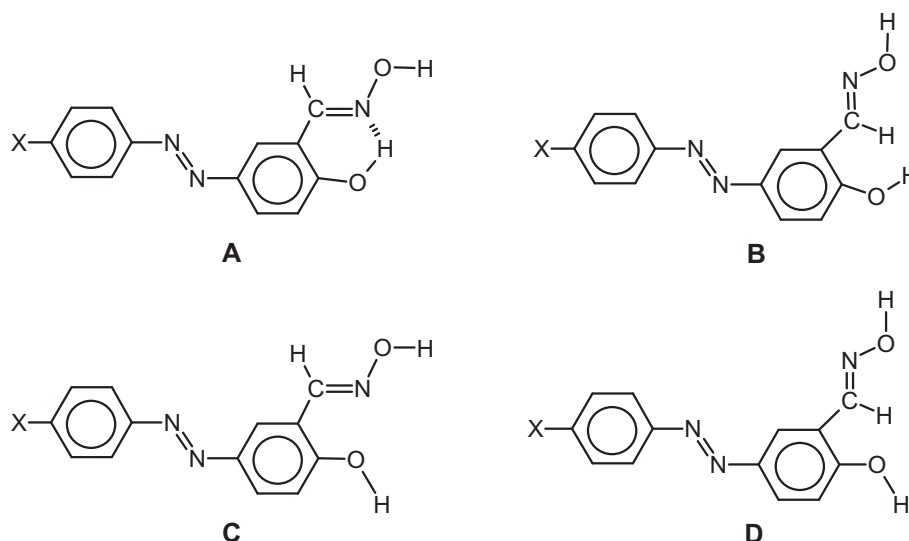


Fig. 1. Possible conformations of oximes.

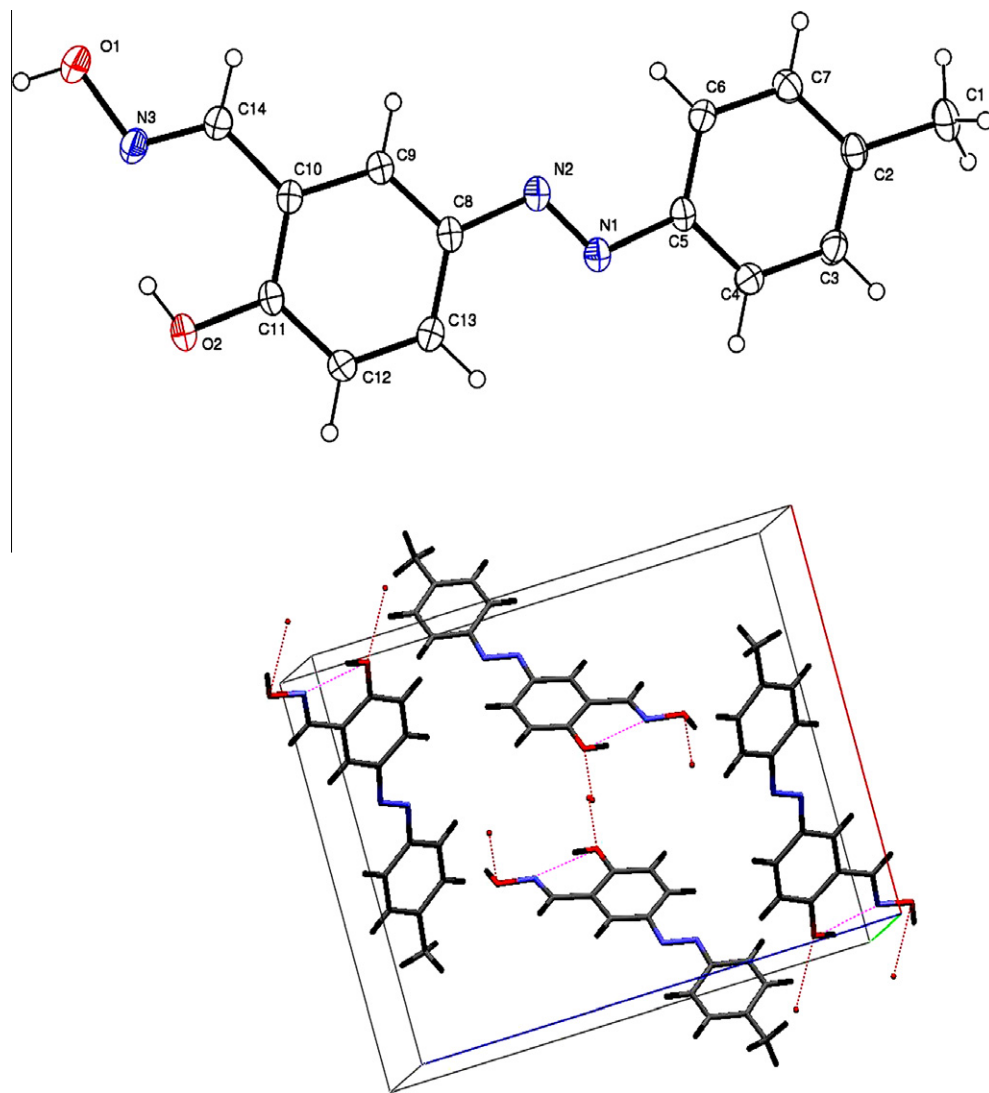


Fig. 2. ORTEP and close packed structures of oxime 7.

arrangement [C(16)—N(17)—O(18)—H(18) torsional angle = 0°]. The barrier is predicted to be 6.98 kcal mol⁻¹. Geometry optimizations were done for the intramolecular hydrogen bonded structures of the other aldehydes and oximes and the optimized structures are reproduced in Fig. 7. To investigate the nature of hydrogen bond, molecular properties such as geometrical parameters, hydrogen bond energies, NBO and AIM parameters have been determined by computational methods.

3.4. Molecular properties

3.4.1. Geometric parameters

From the optimized structures, geometrical parameters were derived and they are compared with the parameters derived from XRD values in the oxime 7 (Table 4) alone. The theoretical bond

lengths are closer to the XRD values. However for the bond angles and torsional angles, deviation is noticed and the maximum deviation in torsional angle is found to be 4°. Selected geometrical parameters which give information about the intramolecular hydrogen bonding are listed in Table 5. The usual geometric parameters related with hydrogen-bonding are the H₁₅···N_{D17}, O_{A15}—H₁₅ and O_{A15}···N_{D17} distances as well as O_{A15}—H₁₅···N_{D17} angle in oximes 6–10 where O_{A15} and N_{D17} are the electron acceptor oxygen and donor nitrogen atoms, respectively. For aldehydes, the geometric parameters related with hydrogen-bonding are the H₁₅···O_{D17}, O_{A15}—H₁₅ and O_{A15}···O_{D17} distances as well as O_{A15}—H₁₅···O_{D17} angle. The cutoff limit generally accepted for the establishment of a hydrogen bond are H₁₅···N_{D17} < 3.0 Å and O_{15A}—H···N_{17D} > 110° [32,33]. Table 5 reveals that these criteria are satisfied in oximes as well as in their respective aldehydes.

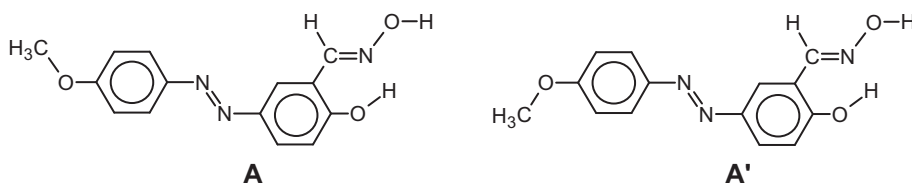


Fig. 3. Possible rotamers of methoxy group in oxime 8.

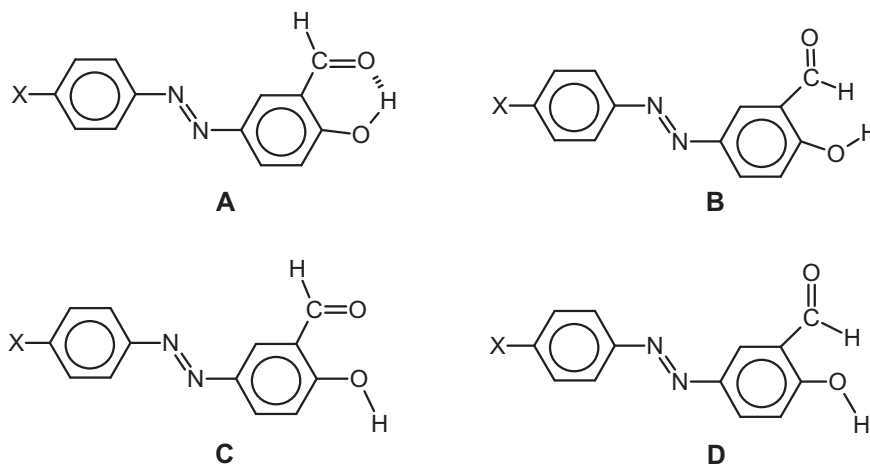


Fig. 4. Possible conformations of aldehydes.

Moreover the distances between the atoms involved in long range interactions depicted in Table 5 are always shorter than the sum of van der Waals radii [34] i.e., the distances observed between the oxygen atom O15 and nitrogen atom N17 in oximes are within the sum of van der Waals radii ($O \cdots N < 307$ pm) and the distances observed between the oxygen atom O15 and oxygen atom O17 in aldehydes is less than 300 pm. Therefore, geometric parameters listed in Table 5 support intramolecular hydrogen bonding in 1–10. The higher $N_{D17} \cdots H_{15}$ and $O_{A15} \cdots N_{D17}$ distances in oximes relative to the $H_{15} \cdots O_{D17}$ and $O_{A15} \cdots O_{D17}$ distances in the parent aldehydes reveal that the extent of intramolecular hydrogen bonding is higher in aldehydes compared to their oximes.

Comparison of energies of a rotamer of a given hydrogen bonded structure with the rotamer with no hydrogen bonding interaction will give an idea of hydrogen bond interaction energies. More specifically rotamer A is compared with the rotamer C for oxime 6 and aldehyde 1. The relative energies are actually the hydrogen bond interaction energies (E_{HB}). For other oximes 7–10 and aldehydes 2–5 energies were determined for rotamers with no hydrogen bonding (Fig. 8) and from comparison with the energies of hydrogen bonded structures (conformation A) hydrogen bond interaction energies were determined and they are also listed in Table 5. The relative energies are not corrected for ZPE differences and may depend on such differences. The higher intramolec-

ular hydrogen bonding interaction in aldehydes compared to their oximes is evidenced from the higher E_{HB} values in aldehydes relative to their oximes.

3.4.2. Natural bond orbital analysis

NBO analysis were carried out for the oximes 6–10 and their parent aldehydes 1–5 and the important second order perturbative estimates of donor–acceptor interactions are displayed in Table 6. The hyperconjugative interaction energies involving C(5) *p*-orbital with the antibonding orbitals of vicinal C(1)–C(6), N(7)–N(8) and C(3)–C(4) bond are found to be very high (≈ 81 , 70 and 69 kcal mol⁻¹) and this is the primary delocalization seen in the oximes 6–9. In the parent aldehydes 1–4 the hyperconjugative interaction energy involving C(1) *p*-orbital with the antibonding orbital of vicinal C(16)–O(17) bond is found to be very high (≈ 77 kcal mol⁻¹) and this is the primary delocalization present in their parent aldehydes 1–4. However in oxime 10 and its parent aldehyde 5 primary delocalization occurs within the orbitals of the nitro group attached to the *para* position of the phenyl ring attached to N(8).

Most stabilizing interactions take place between vicinal NBOs. Besides these some interactions between remote filled and unfilled orbitals are also present. The main stabilized interaction involves the N(17) lone pair as donor and the O(15)–H(15) antibond orbital

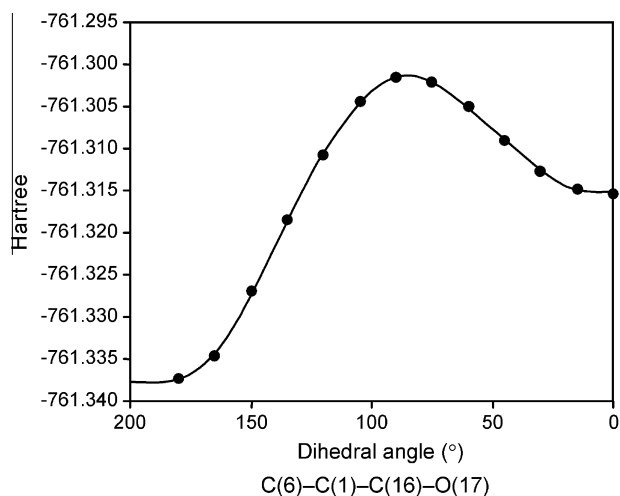


Fig. 5. PES diagram of aldehyde 1.

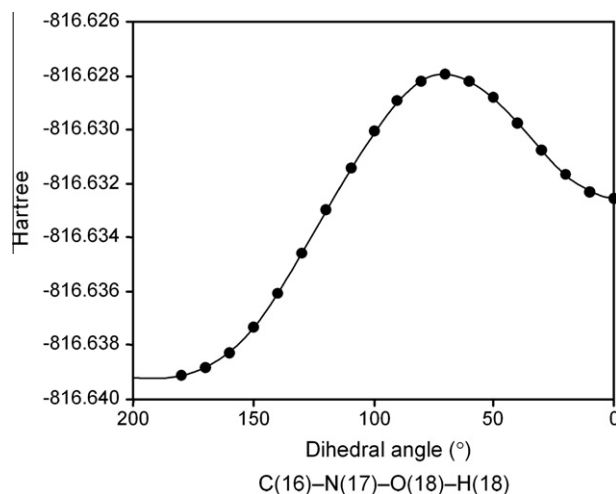


Fig. 6. PES diagram of oxime 6.

$[\sigma^*O(15)-H(15)]$ as acceptor in oximes **6–9** and O(17) lone pair as donors and O(15)–H(15) antibonding orbital $[\sigma^*O(15)-H(15)]$ as acceptor in aldehydes **1–4**. However in oxime **10** and its aldehyde **5** the strong interaction involve N(17)/O(17) lone pair as donor and the antibonding pure *s*-orbital of H(15) $[\sigma^*H(15)]$ as acceptor. The delocalization energy corresponding to the intramolecular hydrogen bonding is slightly lower in oximes than in aldehydes. Among the various substituted compounds studied the nitro derivative is found to have higher stabilizing energy indicating that the intramolecular hydrogen bond formation efficiency is higher in nitro derivatives **5** and **10** compared to other derivatives.

3.4.3. Atoms-in-molecules analysis

Atoms-in-molecules (AIM) electron density topological analyses were carried out for oximes **6–10** and aldehydes **1–5**. Table 7 lists ρ_{BCP} , $\nabla^2\rho_{BCP}$, ϵ , the three eigen values λ_1 , λ_2 and λ_3 , the relationship between the perpendicular and parallel curvatures $|\lambda_1|/|\lambda_3|$, the potential energy density *V*, the kinetic energy density *G*, the total energy density *H* and the kinetic energy density for charge

unit G/ρ_{BCP} values for some selected bonds of oximes and their aldehydes [N7–N8, C2–O15, O15–H15, C16–O17, C16–N17, N17–O18, O18–H18, O17...H15 and N17...H15] and ρ values of ring critical points (RCPs). The negative values obtained for the Laplacian of electron density ($\nabla^2\rho$) for N7–N8, C2–O15, O15–H15, C16–O17, C16–N17, N17–O18 and O18–H18 bonds are a clear indication that the electronic charge is locally concentrated within the region of inter atoms leading to an interaction named as covalent or polarized bonds and being characterized by large ρ values [35–37]. Besides these BCP was located between the non-bonded H(15) and N(17) atoms in oximes and H(15) and O(17) atoms in aldehydes. Popelier proposed that the establishment of a hydrogen bond should be accompanied by four local topological properties of the electron density [38,39]; (i) existence of a (3, –1) BCP between the atoms involved in the interaction, (ii) density at the BCP (ρ_{BCP}) in the range 0.002–0.040 au, (iii) Laplacian of the density at the same point $\nabla^2\rho_{BCP}$ is positive and in the range 0.015–0.15 au and (iv) existence of mutual penetration of hydrogen and the electron-donor atoms nitrogen and oxygen.

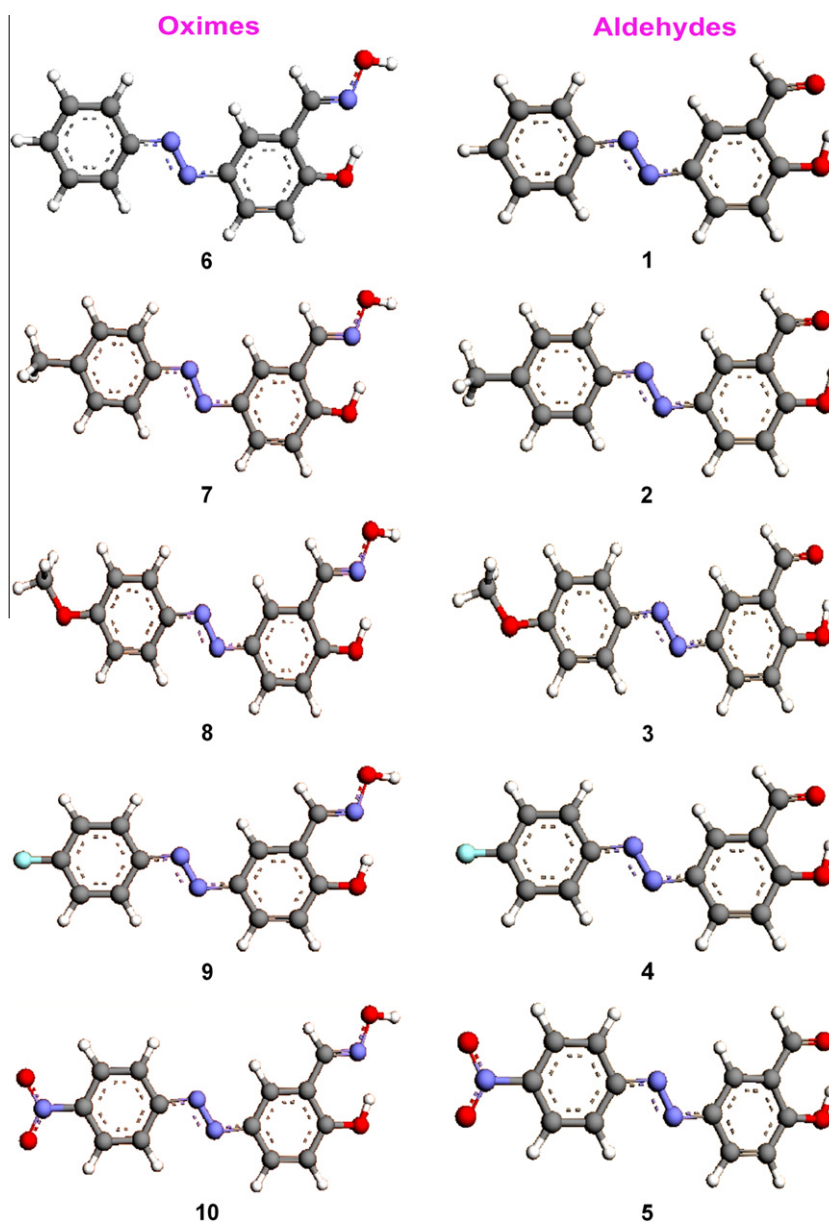


Fig. 7. Optimized structures of oximes **6–10** and their parent aldehydes **1–5**.

Table 4
Selected geometric parameters [bond lengths (Å), bond angles (°) and torsional angles (°)] in oximes **6–10** and their parent aldehydes **1–5**.

Geometric parameters	7		6	8	9	10	1	2	3	4	5
	XRD	Theor.									
<i>Bond length</i>											
C1–C2	1.407	1.426	1.427	1.426	1.427	1.429	1.426	1.437	1.427	1.427	1.428
C1–C6	1.395	1.398	1.400	1.399	1.398	1.396	1.399	1.400	1.400	1.400	1.397
C1–C16	1.455	1.458	1.458	1.457	1.458	1.458	1.455	1.456	1.455	1.456	1.458
C2–C3	1.388	1.402	1.402	1.402	1.402	1.403	1.404	1.404	1.404	1.404	1.405
C2–O15	1.359	1.344	1.343	1.344	1.343	1.340	1.335	1.336	1.337	1.335	1.332
C3–C4	1.378	1.386	1.386	1.386	1.386	1.384	1.384	1.385	1.385	1.384	1.383
C6–C5	1.379	1.399	1.399	1.399	1.399	1.401	1.395	1.395	1.395	1.396	1.397
C5–C4	1.401	1.406	1.406	1.406	1.406	1.408	1.410	1.411	1.411	1.411	1.412
C5–N7	1.427	1.412	1.412	1.412	1.411	1.405	1.413	1.414	1.414	1.413	1.408
N7–N8	1.246	1.263	1.263	1.264	1.263	1.265	1.262	1.263	1.264	1.262	1.263
C16–O17/N17	1.271	1.286	1.286	1.287	1.286	1.286	1.233	1.234	1.234	1.234	1.233
C16–H16	0.930	1.092	1.092	1.092	1.092	1.092	1.106	1.107	1.107	1.107	1.106
N17–O18	1.395	1.397	1.397	1.398	1.397	1.394	–	–	–	–	–
N8–C9	1.428	1.415	1.418	1.411	1.415	1.417	1.417	1.415	1.410	1.415	1.417
C12–X18	1.501	1.509	–	1.361	1.348	1.469	–	1.509	1.360	1.347	1.470
<i>Bond angle</i>											
C2–C1–C16	122.6	121.9	121.9	121.9	121.9	121.9	119.8	119.8	119.8	119.8	119.8
C6–C1–C16	119.2	119.0	119.9	120.0	119.0	119.1	120.3	120.3	120.2	120.3	120.3
C1–C2–O15	121.3	122.3	122.3	122.3	122.3	122.2	121.6	121.6	121.6	121.6	121.5
C3–C2–O15	118.4	118.1	118.1	118.1	118.1	118.1	119.2	119.4	119.2	119.2	119.1
C6–C5–N7	115.4	125.0	124.9	125.0	125.0	124.9	125.1	125.2	125.3	125.2	125.1
C4–C5–N7	125.5	116.1	116.0	116.1	116.0	115.9	116.0	116.0	116.0	115.9	115.9
C2–O15–H15	109.5	108.6	108.6	108.5	108.6	108.7	107.1	107.1	107.1	107.1	107.3
C5–N7–N8	114.1	115.0	115.0	114.9	115.1	115.3	114.8	114.2	114.7	114.8	115.1
C1–C16–N17/O17	124.1	124.1	124.2	124.1	123.9	121.0	121.5	121.4	121.5	121.4	121.2
C16–N17–O18	112.2	112.1	112.1	113.0	112.1	112.2	–	–	–	–	–
N7–N8–C9	113.9	114.9	114.8	115.0	114.8	114.3	115.0	115.0	115.9	115.5	114.4
N8–C9–C10	125.0	125.0	125.8	125.1	124.0	124.7	124.8	125.0	125.1	124.8	124.7
N17–O18–H18	109.5	103.1	103.1	103.1	103.1	103.3	–	–	–	–	–
<i>Torsional angle</i>											
C6–C1–C2–O15	178.7	–180.0	180.0	–180.0	180.0	–180.0	180.0	180.0	180.0	180.0	180.0
C6–C1–C16–N17	–177.4	–180.0	180.0	–180.0	–180.0	–180.0	–	–	–	–	–
C6–C1–C10–O17	–	–	–	–	–	–	180.0	–180.0	180.0	180.0	180.0
C2–C1–C16–N17	2.8	0.0	0.0	0.0	0.0	0.0	–	–	–	–	–
C1–C2–O15–H15	–	0.0	0.0	0.0	0.0	0.0	0.0	0.0	0.0	0.0	0.0
C3–C2–O15–H15	–	–180.0	180.0	–180.0	180.0	–180.0	180.0	–180.0	180.0	180.0	180.0
C16–N17–O18–H18	–	–180.0	–180.0	–180.0	180.0	–180.0	–	–	–	–	–
C1–C16–N17–O18	–179.3	180.0	–180.0	180.0	–180.0	180.0	–	–	–	–	–
C5–N7–N8–C9	–179.4	180.0	–180.0	180.0	180.0	–180.0	180.0	–180.0	180.0	180.0	180.0
N7–N8–C9–C10	3.9	0.0	0.0	0.0	0.0	0.0	0.0	0.0	0.0	0.0	0.0
C1–C16–N17–H15	0.0	0.0	0.0	0.0	0.0	0.0	0.0	0.0	0.0	0.0	0.0
C16–N17–H15–O15	–	0.0	0.0	0.0	0.0	0.0	–	–	–	–	–
C2–O15–H15–N17	–	0.0	0.0	0.0	0.0	0.0	–	–	–	–	–

The ρ_{BCP} values obtained in the present study and positive magnitude of $\nabla^2\rho_{BCP}$ reported in Table 7 are in the high limit of the requirements to define a hydrogen bond and thus a strong interaction may be inferred.

Moreover a ring critical point (RCP) is also observed in both the oximes [C(1)–C(2)–O(15)–H(15)–N(17)–C(16)] and aldehydes [C(1)–C(2)–O(15)–H(15)–O(17)–C(16)] thus reinforcing the idea

of a strong intramolecular hydrogen bond for the oximes and aldehydes. The electron density at RCP is found to be less in oximes than in aldehydes. As pointed by Bader [40,41] a relationship exists between the hydrogen bond strength and the density in the BCP. Comparison of ρ_{BCP} and $\nabla^2\rho_{BCP}$ for the oximes **6–10** and parent aldehydes **1–5** indicate that the values are higher in aldehydes than in oximes. As a consequence the hydrogen bond presents a stronger

Table 5
 E_{HB} and intramolecular hydrogen bonding geometrical parameters in **1–10**.

Comps.	$O_{A15}-H_{15}$ (Å)	$O_{D17}\cdots H_{15}$ (Å)	$O_{D17}\cdots O_{A15}$ (Å)	$O_{A15}-H_{15}\cdots O_{D17}$ (°)	$N_{D17}\cdots H_{15}$ (Å)	$N_{D17}\cdots O_{15A}$ (Å)	$O_{15A}-H_{15}\cdots N_{D17}$ (°)	E_{HB} (kcal mol ⁻¹)
1	0.991	1.723	2.616	147.8	–	–	–	12.171
2	0.991	1.724	2.616	147.8	–	–	–	12.181
3	0.991	1.726	2.617	147.8	–	–	–	12.168
4	0.991	1.723	2.615	147.8	–	–	–	12.145
5	0.991	1.721	2.613	147.6	–	–	–	12.132
6	0.986	–	–	–	1.784	2.653	145.0	10.394
7	XRD –	0.820	–	–	–	1.903	146.6	–
	Theor. –	0.986	–	–	2.653	1.785	145.0	10.380
8	0.985	–	–	–	1.786	2.654	145.0	10.330
9	0.986	–	–	–	1.784	2.652	145.0	10.375
10	0.987	–	–	–	1.777	2.647	145.0	10.464

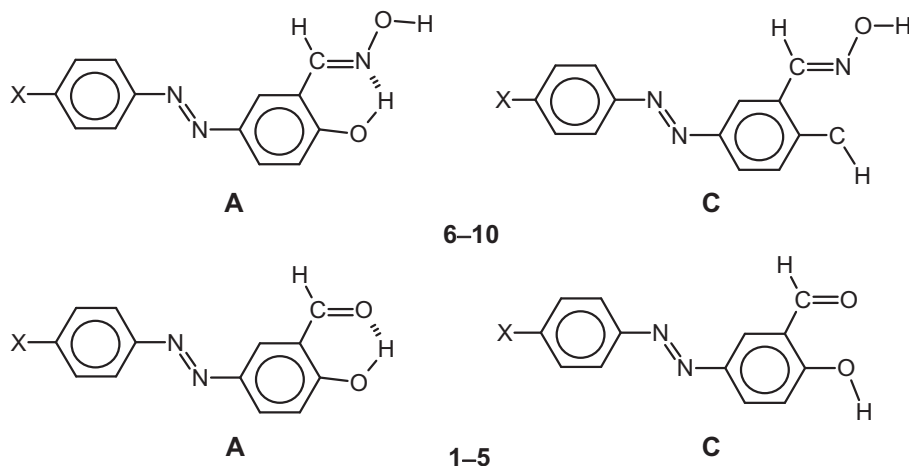


Fig. 8. Conformations of rotamers with and without hydrogen bonding.

Table 6
NBO analysis of **1–10** by DFT method.

Donor NBO	Acceptor NBO	E_2 (kcal mol ⁻¹)									
		1	2	3	4	5	6	7	8	9	10
BD(2)N7–N8	BD*(2)C14–C9	10.48 (10.45)	10.46 (10.41)	10.47 (10.17)	10.46 (10.45)	10.59 (10.55)	10.67 (10.63)	10.66 (10.60)	10.65 (10.59)	10.68 (10.66)	10.66 (10.85)
BD(2)C14–C9	BD*(2)N7–N8	20.62 (21.02)	21.7 (21.74)	22.42 (23.83)	20.87 (21.21)	13.55 (13.74)	20.13 (20.53)	20.76 (21.22)	21.82 (22.29)	20.39 (20.74)	–
BD(2)C6–C5	BD*(2)N7–N8	16.21 (16.46)	16.03 (16.27)	15.87 (16.77)	16.40 (16.69)	22.96 (23.45)	–	–	–	–	–
BD(2)C6–C5	BD*(2)C3–C4	21.92 (22.06)	21.96 (22.10)	21.94 (22.17)	21.87 (22.00)	–	–	–	–	–	–
BD(2)C3–C4	LP*(1)C2	60.96 (61.25)	60.90 (61.17)	60.72 (62.62)	60.86 (61.17)	–	59.94 (60.20)	59.80 (60.06)	59.59 (59.82)	59.84 (60.11)	–
BD(2)C6–C5	LP(1)C1	44.58 (45.13)	44.68 (45.22)	44.84 (44.54)	21.87 (45.08)	–	–	–	–	–	–
LP(2)O15	LP*(1)C2	77.51 (76.09)	77.10 (75.66)	76.49 (72.55)	77.66 (76.28)	77.10 (–)	70.21 (68.99)	69.85 (68.61)	69.27 (68.04)	70.38 (69.19)	–
LP(1)C1	BD*(2)C6–C5	72.22 (72.26)	71.85 (71.89)	71.24 (72.24)	72.46 (72.53)	–	–	–	–	–	–
LP(2)C1	BD*(2)C16–O17	82.31 (77.48)	82.87 (78.02)	83.59 (79.55)	82.04 (77.17)	–	–	–	–	–	–
LP(2)O17/ LP(1)N17	BD*(1)O15–H15	21.25 (17.83)	21.22 (17.80)	21.07 (17.79)	21.23 (17.82)	23.16 (–)	22.37 (17.31)	22.30 (17.24)	22.20 (17.15)	22.41 (17.35)	23.09 (–)
LP(1)N17/O17	LP*(1)H15	–	–	–	–	25.51	–	–	–	–	24.53
BD(2)C1–C6	BD*(2)C16–N17	–	–	–	–	–	24.20 (24.32)	24.7 (24.39)	24.38 (24.51)	24.13 (24.24)	23.67 (23.79)
LP(1)C5	BD*(2)C1–C6	–	–	–	–	–	80.75 (81.10)	81.10 (81.49)	81.69 (82.09)	80.53 (80.83)	–
LP(1)C5	BD*(2)C3–C4	–	–	–	–	–	68.32 (68.74)	68.54 (69.00)	68.78 (69.22)	68.08 (68.46)	–
LP(1)C5	BD*(2)N7–N8	–	–	–	–	–	66.95 (69.48)	66.60 (69.14)	67.03 (69.65)	68.64 (71.42)	–
BD(2)C1–C6	LP*(1)C2	–	–	–	–	–	55.54 (55.80)	55.54 (55.80)	55.42 (55.66)	55.38 (55.65)	–
BD(2)C1–C6	LP*(1)C5	–	–	–	–	–	39.74 (39.95)	39.77 (39.99)	39.87 (40.10)	39.79 (40.02)	–
BD(2)C3–C4	LP(1)C5	–	–	–	–	–	39.33 (39.66)	39.30 (39.62)	39.31 (39.64)	39.38 (39.72)	–
BD(2)N7–N8	LP(1)C5	–	–	–	–	–	17.81 (17.70)	17.94 (17.84)	18.14 (18.03)	17.75 (17.62)	–
LP(2)O19	BD*(2)N18–O20	–	–	–	–	163.76 (163.43)	–	–	–	–	163.30 (162.95)
BD(2)C1–C6	BD*(2)C16–O17/ N17	–	–	–	–	28.79 (27.68)	–	–	–	–	23.79 (23.67)
BD(2)C5–C4	BD*(2)N7–N8	–	–	–	–	16.03 (23.85)	–	–	–	–	2.10 (24.31)
LP(3)O15	LP*(1)H15	–	–	–	–	438.52	–	–	–	–	485.38

Values within parentheses are the values derived from B3LYP/6-311+G(d,p).
Bold values indicates intramolecular hydrogen bonding parameters.

interaction in aldehydes than in oximes. This is also in line with the distances observed between the oxygen atom O15 and oxygen atom

O17 in aldehydes (lower values) and the distances between the oxygen atom O15 and nitrogen atom N17 in oximes (higher values).

Table 7
Topological properties at BCP (3, -1) in relevant bonds of **1-10**.

Compds.	Bond (A...B)	ρ_{BCP}	$-\nabla^2\rho_{BCP}$	ε	λ_1	λ_2	λ_3	$ \lambda_1 /\lambda_3$	G	V	H	G_b/ρ_{BCP}
1	N ₇ -N ₈	0.4547	1.0452	0.1330	-1.0870	-0.9594	1.0012	1.0857	0.2742	-0.8097	-0.5355	0.6031
	C ₂ ...O ₁₅	0.3103	0.3507	0.0025	-0.6715	-0.6698	0.9906	0.6779	0.4033	-0.8943	-0.4910	1.2998
	O ₁₅ ...H ₁₅	0.3342	1.9319	0.0164	-1.7538	-1.7254	1.5473	1.1334	0.0719	-0.6268	-0.5549	0.2152
	C ₁₆ -O ₁₇	0.3889	-0.1512	0.0433	-0.9923	-0.9511	2.0946	0.4737	0.6893	-1.3408	-0.6515	1.7723
2	O ₁₇ ...H ₁₅	0.0455	-0.1290	0.0008	-0.0733	0.0733	0.2756	0.2660	0.0341	-0.0359	-0.0018	0.7494
	N ₇ -N ₈	0.4170	0.8030	0.0903	-1.0021	-0.9191	1.1182	0.8962	0.2260	-0.6528	-0.4268	0.5420
	C ₂ ...O ₁₅	0.2910	0.5107	0.1518	-0.6259	-0.5434	0.6587	0.9502	0.2930	-0.7138	-0.4208	1.0068
	O ₁₅ ...H ₁₅	0.3089	1.4972	0.0188	-1.4867	-1.4594	1.4489	1.0261	0.0566	-0.4874	-0.4308	0.1831
3	C ₁₆ -O ₁₇	-0.3698	3.1890	0.1108	-0.9290	-0.8363	1.4463	0.6423	0.5220	-1.1237	-0.6017	1.4115
	O ₁₇ ...H ₁₅	-0.4436	0.1619	0.0028	-0.0734	-0.0732	0.3085	0.2380	0.0425	-0.0446	-0.0021	0.0958
	N ₇ -N ₈	0.4523	1.0340	0.1340	-1.0799	-0.9523	0.9981	1.0820	0.2720	-0.8025	-0.5305	0.6014
	C ₂ ...O ₁₅	0.3095	0.3527	0.0013	-0.6676	-0.6667	0.9816	0.6801	0.4009	-0.8901	-0.4892	1.2948
4	O ₁₅ ...H ₁₅	0.3347	1.9353	0.0166	-1.7563	-1.7276	1.5486	1.1341	0.0720	-0.6279	-0.5559	0.2152
	C ₁₆ -O ₁₇	0.3887	-0.1488	0.0430	-0.9911	-0.9502	2.0901	0.4742	0.6882	-1.3392	-0.7510	1.7706
	O ₁₇ ...H ₁₅	0.0453	-0.1285	0.0001	-0.0727	-0.0727	0.2739	0.2654	0.0339	-0.0357	-0.0018	0.7483
	N ₇ -N ₈	0.4542	1.0427	0.1340	-1.0856	-0.9573	1.0002	1.0854	0.2738	0.8083	-0.5345	0.6029
5	C ₂ ...O ₁₅	0.3105	0.3499	0.0022	-0.6721	-0.6706	0.9928	0.6770	0.4039	-0.8954	-0.4915	1.3008
	O ₁₅ ...H ₁₅	0.3343	1.9330	0.0164	-1.7548	-1.7265	1.5481	1.1335	0.0719	-0.6271	-0.5552	0.2151
	C ₁₆ -O ₁₇	0.3891	-0.1522	0.0435	-0.9928	-0.9515	2.0965	0.4736	0.6898	-1.3416	-0.6518	1.7728
	O ₁₇ ...H ₁₅	0.0455	-0.1290	0.0007	-0.0733	-0.0733	0.2660	0.2660	0.0341	-0.0359	0.0018	0.7494
6	N ₇ -N ₈	0.4536	1.0426	0.1295	-1.0839	-0.9596	1.0008	1.0830	0.2726	-0.8059	-0.5333	0.6010
	C ₂ ...O ₁₅	0.3123	0.3426	0.0042	-0.6802	-0.6774	1.0150	0.6702	0.4098	-0.9052	-0.4954	1.3120
	O ₁₅ ...H ₁₅	0.3335	1.9302	0.0160	-1.7525	-1.7249	1.5472	1.1326	0.0715	-0.6256	-0.5541	0.2143
	C ₁₆ -O ₁₇	0.3898	-0.1598	0.0444	-0.9964	-0.9540	2.1102	0.4717	0.6932	-1.3465	-0.6533	1.7783
7	O ₁₇ ...H ₁₅	0.0456	-0.1294	0.0001	-0.0738	-0.0738	0.2770	0.2669	0.0342	-0.0361	-0.0019	0.7493
	N ₇ -N ₈	0.4540	1.0422	0.1327	-1.0849	-0.9578	1.0005	1.0843	0.2735	-0.8076	-0.5341	0.6024
	C ₂ ...O ₁₅	0.3037	0.3454	0.0055	-0.6457	-0.6421	0.9425	0.6850	0.3898	-0.8659	-0.4761	1.2836
	O ₁₅ ...H ₁₅	0.3399	1.9600	0.0177	-1.7775	-1.7465	1.5639	1.1366	0.0741	-0.6382	-0.5641	0.2180
8	C ₁₆ -N ₁₇	0.3755	0.5326	0.2610	-0.8904	-0.7061	1.0639	0.8369	0.5152	-1.1636	-0.6484	1.3720
	N ₁₇ ...H ₁₅	0.0421	-0.1085	0.0417	-0.0646	-0.0620	0.2352	0.2747	0.0291	-0.0310	-0.0019	0.6912
	H ₁₈ -O ₁₈	0.3682	2.1332	0.0366	-1.8935	-1.8266	1.5869	1.1932	0.0729	-0.6790	-0.6061	0.1978
	N ₁₇ -O ₁₈	0.3201	0.4350	0.0569	-0.7329	-0.6935	0.9914	0.7393	0.1940	-0.4968	-0.3028	0.6061
9	N ₇ -N ₈	0.4533	1.0391	0.1329	-1.0829	-0.9559	0.9998	1.0830	0.2729	-0.8056	-0.5327	0.6020
	C ₂ ...O ₁₅	0.3034	0.3458	0.0060	-0.6446	-0.6408	0.9396	0.6861	0.3890	-0.8645	-0.4755	1.2823
	O ₁₅ ...H ₁₅	0.3400	1.9605	0.0178	-1.7777	-1.7466	1.5638	1.1368	0.0741	-0.6384	-0.5643	0.2181
	C ₁₆ -N ₁₇	0.3754	0.5333	0.2605	-0.8902	-0.7062	1.0631	0.8373	0.5150	-1.1633	-0.6483	1.3718
10	N ₁₇ ...H ₁₅	0.0420	-0.1084	0.0418	-0.0644	-0.0618	0.2347	0.2746	0.0290	-0.0309	-0.0019	0.6905
	H ₁₈ -O ₁₈	0.3682	2.1323	0.0367	-1.8928	-1.8258	1.5863	1.1932	0.0729	-0.6789	-0.6060	0.1980
	N ₁₇ -O ₁₈	0.3198	0.4335	0.0569	-0.7319	-0.6925	0.9909	0.7386	0.1938	-0.4960	-0.3022	0.6061
	N ₇ -N ₈	0.4519	1.0322	0.1338	-1.0786	-0.9513	0.9978	1.0810	0.2717	-0.8014	-0.5297	0.6012
11	C ₂ ...O ₁₅	0.3028	0.3474	0.0069	-0.6436	-0.6382	0.9334	0.6895	0.3874	-0.8616	-0.4742	1.2793
	O ₁₅ ...H ₁₅	0.3403	1.9620	0.0179	-1.7788	-1.7474	1.5643	1.1372	0.0742	-0.6390	-0.5648	0.2181
	C ₁₆ -N ₁₇	0.3753	0.5349	0.2597	-0.8896	-0.7062	1.0609	0.8385	0.5143	-1.1624	-0.6481	1.3704
	N ₁₇ ...H ₁₅	0.0419	-0.1083	0.0421	-0.0642	-0.0616	0.2341	0.2742	0.0290	-0.0308	0.0018	0.6921
12	H ₁₈ -O ₁₈	0.3683	2.1317	0.0367	-1.8923	-1.8252	1.5858	1.1932	0.0730	-0.6789	-0.6059	0.1982
	N ₁₇ -O ₁₈	0.3193	0.4314	0.0569	-0.7303	-0.6910	0.9900	0.7377	0.1935	-0.4948	-0.3013	0.6061
	N ₇ -N ₈	0.4533	1.0389	0.1337	-1.0831	-0.9553	0.9995	1.0884	0.2730	-0.8058	-0.5328	0.6023
	C ₂ ...O ₁₅	0.3039	0.3447	0.0057	-0.6465	-0.6429	0.9447	0.6844	0.3904	-0.8670	-0.4766	1.2848
13	O ₁₅ ...H ₁₅	0.3397	1.9590	0.0177	-1.7767	-1.7458	1.5635	1.1364	0.0741	-0.6379	-0.5638	0.2181
	C ₁₆ -N ₁₇	0.3754	0.5329	0.2615	-0.8904	-0.7058	1.0633	0.8374	0.5151	-1.1634	-0.6483	1.3721
	N ₁₇ ...H ₁₅	0.0421	-0.1086	0.0416	-0.0647	-0.0622	0.2355	0.2750	0.0291	-0.0310	-0.0031	0.6912
	H ₁₈ -O ₁₈	0.3682	2.1336	0.0366	-1.8938	-1.8269	1.5872	1.1932	0.0728	-0.6790	-0.6062	0.1977
14	N ₁₇ -O ₁₈	0.3203	0.4359	0.0569	-0.7336	-0.6941	0.9918	0.7397	0.1941	-0.4973	-0.3032	0.6061
	N ₇ -N ₈	0.4521	1.0359	0.1285	-1.0791	-0.9562	0.9993	1.0800	0.2711	-0.8011	-0.5300	0.5996
	C ₂ ...O ₁₅	0.3061	0.3371	0.0030	-0.6547	-0.6527	0.9703	0.6747	0.3973	-0.8788	-0.4815	1.2979
	O ₁₅ ...H ₁₅	0.3384	1.9509	0.0172	-1.7712	-1.7413	1.5616	1.1342	0.0738	-0.6353	-0.5615	0.2181
15	C ₁₆ -N ₁₇	0.3756	0.5287	0.2648	-0.8914	-0.7048	1.0676	0.8350	0.5164	-1.1649	-0.6485	1.3747
	N ₁₇ ...H ₁₅	0.0429	-0.1097	0.0406	-0.0665	-0.0639	0.2400	0.2769	0.0295	-0.0316	0.0021	0.6876
	H ₁₈ -O ₁₈	0.3679	2.1357	0.0364	-1.8956	-1.8290	1.5889	1.1930	0.0724	-0.6787	-0.6063	0.1967
	N ₁₇ -O ₁₈	0.3225	0.4450	0.0572	-0.7402	-0.7002	0.9954	0.7436	0.1955	-0.5022	-0.3067	0.6062

The energetic properties of BCP associated with the intramolecular hydrogen bonding also provide valuable information about the characteristics of this interaction. Kinetic energy density G , is always positive and its ratio to electron density (G/ρ_{BCP}) may be used to define the character of the interaction. This ratio may be larger than 1.0 for closed shell (hydrogen bonding, ionic bonds and van der Waals interaction) and less than 1.0 for shared interactions (covalent bonds) [35]. The ratio G/ρ_{BCP} reported in Table 7 is lower than 1.0 for the intramolecular hydrogen bonding, although for closed shell interactions as these ones should be larger than 1.0. Nevertheless values slightly lower than 1.0 have been reported for remarkably strong hydrogen bonding in other compounds

[42,43]. H value is almost null pointing again to strong hydrogen bond. As a rule the larger the G values, the stronger the interaction and thus a strong intramolecular hydrogen bond may be inferred from the values reported in Table 7. The critical point found in the intramolecular hydrogen bond has two negative (λ_1 and λ_2) and one positive eigen values (λ_3). The relationship between the negative and positive curvatures $|\lambda_1|/\lambda_3$ is less than 1.0, as it generally occurs in an hydrogen bond interaction [37].

3.4.4. Dipole moments and polarizabilities

The dipole moments, polarizabilities and first order polarizabilities were also calculated by finite field approach using the basis

Table 8

Dipole moment $\mu(D)$, polarizability ($\alpha_{\text{tot}} \times 10^{23}$ esu) and hyperpolarizability ($\beta_{\text{tot}} \times 10^{33}$ esu) for oximes **6–10** and their parent aldehydes **1–5**.

Comps.	Dipole moment	Polarizability	Hyperpolarizability
6	1.26	30.448	22340.68
7	1.13	33.222	16377.74
8	2.66	34.766	1502.71
9	2.18	31.800	16109.50
10	7.06	35.549	89263.27
1	2.76	27.853	13141.49
2	3.51	30.614	6598.80
3	4.57	32.218	9710.80
4	1.47	28.217	7011.95
5	3.46	32.471	65781.88

set B3LYP/6-31G* available in Gaussian-03 package and these values are listed in Table 8. In compounds containing electron-withdrawing substituents (nitro and fluoro) the dipole moment is increased due to oximation, whereas in other compounds oximation decreases the dipole moment. Oximation increases both the polarizability and hyperpolarizability values.

4. Conclusions

Structures of 5-arylazosalicylaloximes **6–10** are arrived from spectral and theoretical analysis. Single crystal XRD measurements were made for 5-*p*-tolylazosalicylaloxime (**7**). AIM, NBO and selected geometric parameters are used as tools to predict the nature of intramolecular hydrogen bonding in aldehydes **1–5** and their oximes **6–10**.

Acknowledgement

The authors thank the NMR Research Centre, Indian Institute of Science, Bangalore for recording the NMR spectra.

Appendix A. Supplementary material

IR, ^1H and ^{13}C NMR spectra (Figs. S1–S3) for the oxime **6** are provided. Supplementary data associated with this article can be found, in the online version, at <http://dx.doi.org/10.1016/j.molstruc.2012.06.012>.

References

- [1] H. Rau, in: J.F. Rabek (Ed.), Photochemistry and Photophysics, vol. 2, CRC Press, Boca Raton, Florida, 1990, p. 119.
- [2] H. Zollinger, Colour Chemistry, Synthesis, Properties and Application of Organic Dyes, VCH, Weinheim, 1987.
- [3] L.K. Ravindranath, S.R. Ramadas, S.B. Rao, Electrochim. Acta 28 (1983) 601.
- [4] H.G. Garg, R.A. Sharma, J. Med. Chem. 12 (1996) 1122.
- [5] S. Ameerunisha, P.S. Zacharias, J. Chem. Soc. Perk. Trans. 2 (1995) 1679.
- [6] S. Shinkai, T. Nakaji, T. Ogawa, K. Shigematsu, O. Manabe, J. Am. Chem. Soc. 103 (1981) 111.
- [7] V. Padmini, Arch. Appl. Sci. Res. 2 (2010) 356.
- [8] N. Kurtoglu, J. Serb. Chem. Soc. 74 (2009) 917.
- [9] A.S. Burlov, S.A. Nikolaevskii, A.S. Bogomyarov, I.S. Vasil'chenko, Y.V. Koshchchenko, V.G. Vlasenko, A.I. Uraev, D.A. Garnovskii, E.V. Sennikova, G.S. Borodkin, A.D. Garnovskii, V.I. Minkin, Russ. J. Coord. Chem. 35 (2009) 486.
- [10] A.D. Garnovskii, A.S. Burlov, A.G. Starikov, A.V. Metelitsa, I.S. Vasil'chenko, S.O. Bezugliy, S.A. Nikolaevskii, I.G. Borodkina, V.I. Minkin, Russ. J. Chem. 36 (2010) 479.
- [11] M. Han, M. Hara, J. Am. Chem. Soc. 127 (2005) 10951.
- [12] M.R. Han, Y. Hirayama, M. Hara, Chem. Mater. 18 (2006) 2784.
- [13] (a) Z. Sekkat, W. Knoll (Eds.), Photoreactive Organic Thinfilms, Academic Press, Elsevier, 2002;
(b) H. Rau, Angew. Chem., Int. Ed. 12 (1972) 224;
(c) C.G. Morgante, W.S. Struve, Chem. Phys. Lett. 68 (1979) 267.
- [14] R. Weber, B. Winter, I.V. Hertel, B. Stiller, S. Schrader, L. Brehmer, N. Koch, J. Phys. Chem. B 107 (2003) 7768.
- [15] H. Akiyama, K. Tamada, J. Nagasawa, K. Abe, T. Tamaki, J. Phys. Chem. B 107 (2003) 130.
- [16] M. Shimomura, T. Kunitake, J. Am. Chem. Soc. 109 (1987) 5175.
- [17] V. Ramamurthy, D.F. Eaton, J. Chem. Mater. 6 (1994) 1128.
- [18] N. Herron, J. Inclus. Phenom. Mol. Recogn. Chem. 21 (1995) 283.
- [19] N. Gfeller, S. Magelski, G. Calzaferri, J. Phys. Chem. B 102 (1998) 2483.
- [20] A. Corma, H. Garcia, S. Ibarra, V. Marti, M.A. Miranda, J. Primo, J. Am. Chem. Soc. 115 (1993) 2177.
- [21] K. Hoffman, F. Marlow, J. Caro, J. Adv. Mater. 9 (1997) 575.
- [22] (a) K.D. Singer, M.G. Kuzyk, W.R. Holland, J.E. Sohn, S.J. Lalama, R.B. Comizzoli, H.E. Kalz, M.L. Schilling, Appl. Phys. Lett. 52 (1988) 1800;
(b) H.L. Hampsch, J. Yang, G.K. Wong, J.M. Torkelson, Macromolecules 21 (1988) 526;
(c) H.I. Hampsh, J. Yang, G.K. Wong, J.M. Torkelson, Polym. Commun. 30 (1989) 40;
(d) P. Pantelis, J.R. Hill, S.N. Oliver, G.J. Davies, Brit. Telecom. Technol. J. 6 (1988) 5.
- [23] M.L. Schilling, H.E. Kalz, Chem. Mater. 1 (1989) 668.
- [24] S. Yokoyama, S. Mashiko, Mater. Res. Soc. Symp. Proc. 488 (1998) 765.
- [25] S. Yokoyama, T. Nakahama, A. Otomo, S. Mashiko, Thin Solid Films 331 (1998) 248.
- [26] S. Yokoyama, T. Nakahama, A. Otomo, S. Meshiko, J. Am. Chem. Soc. 122 (2000) 3174.
- [27] Y. Okuno, S. Yokoyama, S. Mashiko, J. Phys. Chem. B 105 (2001) 2163.
- [28] M. Odabasoglu, C. Albayrak, R. Ozkanca, F.Z. Aykan, P. Lonecke, J. Mol. Struct. 840 (2007) 71.
- [29] M.J. Frisch, G.W. Trucks, H.B. Schlegel, G.E. Scuseria, M.A. Robb, J.R. Cheeseman, V.G. Zakrzewski, J.A. Montgomery Jr., R.E. Stratmann, J.C. Burant, S. Dapprich, J.M. Millam, A.D. Daniels, K.N. Kudin, M.C. Strain, O. Farkas, J. Tomasa, V. Barone, M. Cossi, R. Cammi, B. Mennucci, C. Pomeli, C. Adamo, S. Clifford, J. Ochterski, G.A. Peterson, P.Y. Ayala, Q. Cui, K. Morokuma, P. Salvador, J.J. Dannenberg, D.K. Malick, A.D. Rabuck, K. Raghavachari, J.B. Poresman, J. Cioslowski, J.N. Ortiz, A.G. Babboul, B.B. Stefanov, G. Liu, A. Liashenko, P. Piskorz, I. Komaromi, R. Gomperts, R.L. Martin, D.J. Fox, T. Keith, M.A. Allaham, C.Y. Peng, A. Nanayakkara, M.W. Wong, J.L. Anders, C. Gonzales, M. Challacombe, P.M. Gill, B. Johnson, W. Chen, M. Head-Gordon, E.S. Replogle, J.A. Pople, Gaussian 98, Revision A. 9, Pittsburg, Pa, Gaussian IC, 2001.
- [30] T.A. Keith, AIM All (Version 11.04.03) (aim.tkgriskmill.com), 2011.
- [31] G.M. Sheldrick, Acta Crystallogr. A 64 (2008) 112.
- [32] T. Steiner, Angew. Chem. Int. Ed. 41 (2002) 48.
- [33] G.A. Jeffrey, An Introduction of Hydrogen Bonding, Oxford University Press, Oxford, 2002.
- [34] A. Bondi, J. Phys. Chem. 68 (1964) 441.
- [35] R.F.W. Bader, Atoms in Molecules: A Quantum Theory, Oxford University Press, Oxford, 1990.
- [36] R.F.W. Bader, Chem. Rev. 91 (1991) 893.
- [37] N.G. Fidanza, G.L. Sosa, R.M. Lobayan, N.M. Peruchena, J. Mol. Struct. (Theochem) 722 (2005) 65.
- [38] U. Koch, P.L.A. Popelier, J. Phys. Chem. 99 (1995) 9747.
- [39] L.F. Pacios, P.C. Gomez, J. Comput. Chem. 22 (2001) 702.
- [40] M.T. Caroll, R.F.W. Bader, Mol. Phys. 65 (1988) 695.
- [41] M.T. Caroll, C. Chang, R.F.W. Bader, Mol. Phys. 63 (1988) 387.
- [42] D.E. Hibbs, J. Overgaard, R.O. Plitz, Org. Biomol. Chem. 1 (2003) 1191.
- [43] S. Aparicio, R. Alcaldo, Eur. J. Chem. 3 (2010) 162.